Flux Saturation Model Using Arctangent and Logarithm Functions Considering the Flux Characteristics of Synchronous Reluctance Machines

Tae-gyeom Woo[1], Hyun-Jun Lee[2], Young-Doo Yoon[2]
[1] Department of Automotive Engineering(Automotive-Computer Convergence), Hanyang University, Korea
[2] Department of Automotive Engineering, Hanyang University, Korea

***Abstract*--** This paper describes a flux saturation model expressing the current and flux relationship. The flux saturation model includes a self-saturation term and a cross-saturation term. The flux saturation of the synchronous reluctance machine was analyzed and based on this, the self-saturation term was selected, and the cross-saturation term was proposed. The self-saturation term is an arctangent function that can represent the nonlinear flux saturation well. And the cross-saturation term was proposed considering the cross-saturation and the reciprocity condition. The proposed flux saturation model was experimentally verified for flux saturation of 1.5 kW SynRM.

***Index Terms*—self-commissioning method, self-saturation, cross-saturation, flux saturation model**

I. INTRODUCTION

Synchronous reluctance machines (SynRMs) are low-cost and high-temperature robust [1]-[3]. However, a high salient ratio and large inductance are required to obtain high output torque because this motor does not have a permanent magnet. In addition, flux saturation [4] occurs significantly due to volume reduction to obtain high power density.

Flux saturation modeling is essential to achieve good control performance. Flux saturation data obtained through finite element analysis (FEA) or experiments are required for estimating flux saturation model. Information on the drawings and materials of the motor is required for FEA. However, when there is no such motor information, flux saturation data can be obtained through a self-identification process.

The self-identification method is divided into a rotating state or a stationary state [5]. The self-identification method in the rotating state obtains flux saturation data through current control. Because of the current control, flux saturation data with respect to the desired currents can be obtained. Also, a position sensor is required for speed control. The self-identification method in the stationary state obtains flux saturation data using a hysteresis voltage injection technique. The hysteresis voltage injection technique injects voltage so that the current pulsates within the current limit. This method obtains flux saturation data with respect to the currents within the current limit. And since flux saturation data is obtained in a stationary state, a load system is not required.

Flux saturation modeling methods include tables [6], artificial neural networks (ANNs) [7,8], and equations [9]-[15]. The table-based flux saturation modeling method requires flux data for each row and column. The ANN and equation-based flux saturation modeling method improves the modeling accuracy as uniformly distributed flux data is obtained. However, in the ANN-based flux saturation modeling method, the flux error between the ANN model and the non-learning area may be significantly different when the flux data for learning is insufficient. However, the equation-based flux saturation modeling method can also represent the flux region not used to estimate the flux saturation model well. Therefore, table- and ANN-based flux saturation modeling using the flux data obtained by the self-identification process of the rotating state is suitable for systems with load system. Equation-based flux saturation modeling using flux data obtained in the self-identification process in a stationary state is suitable for cases without a load system.

Many equation-based flux models have been studied. Equation-based flux saturation models include a current model [9,10] with respect to flux and a flux model [11]-[14] with respect to current. A model that expresses the current with respect to flux well has already been developed. However, there is a lack of research on a flux saturation model that well expresses flux with respect to current.

This paper analyzes the flux saturation phenomenon and proposes a flux saturation model for current based on this. Flux saturation is divided into self-saturation by only its self-axis current and cross-saturation by orthogonal axis current. And the proposed flux saturation model includes self-saturation and cross-saturation terms. The self-

saturation terms are selected as an arctangent function and a linear function considering the nonlinear self-saturation phenomenon. And the cross-saturation term was proposed as a logarithm function considering the cross-saturation phenomenon caused by the orthogonal axis current and the reciprocity condition [9].

The flux saturation data were obtained through a stationary state self-commissioning process. The d- and q-axis self-saturation data were obtained by injecting the d- and q-axis voltages, respectively. Then, the d-q axis voltages were simultaneously injected to obtain cross-saturation data. Based on the flux saturation data, the parameters of the self-saturation term and the cross-saturation term were sequentially estimated. MATLAB's curve-fitting tool was used for parameter estimation of proposed flux saturation model.

This paper analyzes the flux saturation phenomenon of SynRM and proposes an equation-based flux saturation model based on it. Section II explains the fundamental equations. Section III describes the flux saturation phenomenon, and section IV describes the proposed flux saturation model considering the reciprocity condition. Section V experimentally verifies the proposed flux saturation model for a 1.5 kW SynRM.

II. Fundamental Equations

The stator voltage equations of the SynRM model in rotor coordinates are given by

$$u_d = R_s i_d + \frac{d\psi_d}{dt} - \omega_r \psi_q \tag{1a}$$

$$u_q = R_s i_q + \frac{d\psi_q}{dt} + \omega_r \psi_d, \tag{1b}$$

where ψ_d and ψ_q are the flux components, u_d and u_q are the stator voltage components, R_s is the stator resistance, i_d and i_q are the current components, and ω_r is the electrical angular speed of the rotor.

The flux with respect to the d-q axis current is expressed as

$$\psi_d = \psi_d(i_d, i_q), \psi_q = \psi_q(i_d, i_q). \tag{2}$$

The flux function to represent flux saturation is nonlinear, and when electrical energy is neither generated nor dissipated by the inductors, the reciprocity condition [XX] is

$$\frac{d\psi_d(i_d, i_q)}{di_q} = \frac{d\psi_q(i_d, i_q)}{di_d}. \tag{3}$$

The electromagnetic torque is given by

$$T_e = 1.5pp(\psi_d i_q - \psi_q i_d). \tag{4}$$

where pp is the number of pole pairs.

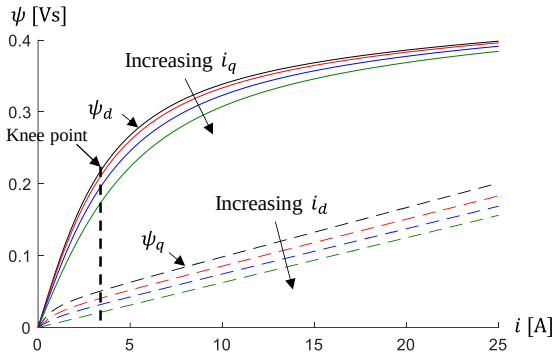

Fig. 1: D-q axis flux saturation of SynRM.

III. Flux Saturation Phenomenon

A. Self-saturation Phenomenon

The d-axis flux is much greater than the q-axis flux because the SynRM is designed to have a high saliency ratio. The solid black line is the d-axis self-saturation, and the black dotted line is the q-axis self-saturation, as shown in Fig.1. Since the q-axis flux is small, there is almost no flux saturation. On the other hand, the d-axis flux changes linearly in the region where the d-axis current is small, and as the d-axis current increases, non-linear flux saturation appears.

B. Cross-saturation Phenomenon

The solid line in Fig. 1 shows the d-axis flux saturation. When the q-axis current is a constant value other than zero, the cross-saturation of the d-axis flux increases as the d-axis current increases, but decreases after the cross-saturation reaches a maximum. The dotted line in Fig. 1 shows the q-axis flux saturation. When the d-axis current is a constant value other than zero, the cross-saturation of the q-axis flux increases as the q-axis current increases.

IV. Proposed Flux Saturation Model

As mentioned in the section III, flux saturation is divided into self-saturation and cross-saturation. The proposed flux saturation model consists of a self-saturation term and a cross-saturation term. Each term was selected and proposed considering the flux saturation phenomenon. The selected self-saturation term involved an arctangent function and linear function, and the proposed cross-saturation terms are a logarithm function. This section explains the physical meaning of the parameters of the proposed flux saturation model.

A. Self-saturation Term

The selected self-saturation model [12] consists of two functions and three parameters, and the d-axis and q-axis self-saturation model is expressed as

$$\psi_d(i_d) = A_d \tan^{-1}(B_d i_d) + C_d i_d, \tag{5a}$$

$$\psi_q(i_q) = A_q \tan^{-1}(B_q i_q) + C_q i_q, \tag{5b}$$

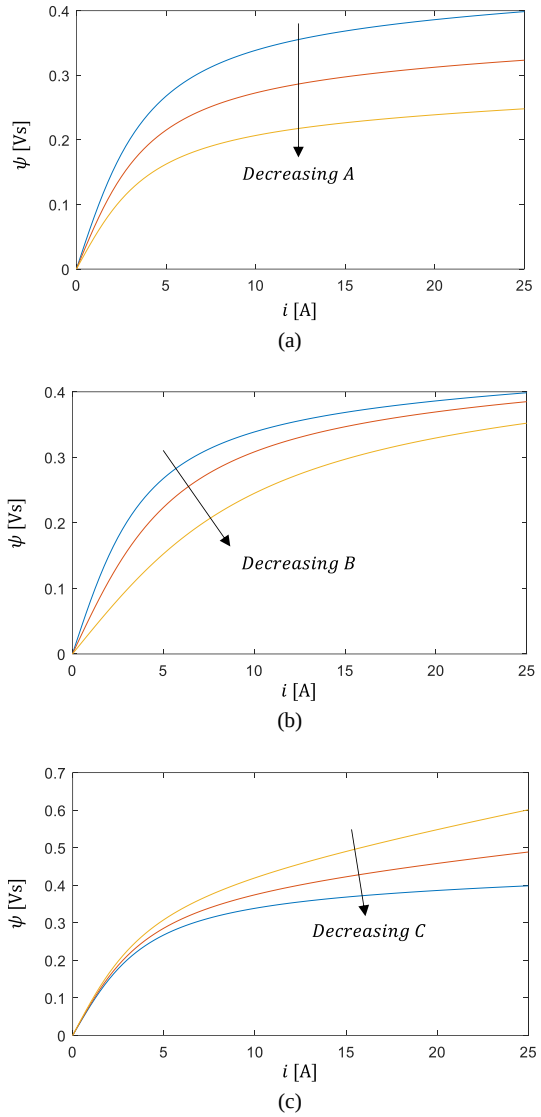

Fig. 2: Examples of self-saturation model with parameter changes: (a) A; (b) B; (c) C.

where A_d, B_d, and C_d are nonnegative coefficients. A_d determines the magnitude of the arctangent function. B_d represent the smoothness of the section from the linear region to the saturated region and the slope of the linear region, respectively.

Fig. 2 shows examples of self-saturation term along A, B, and C. Fig.2(a) shows that the overall magnitude of the flux decreases as A decreases. Fig.2(b) shows that the flux saturation according to the current weakens as B decreases. Fig. 2(c) shows that the slope of the saturation region decreases as C decreases. Therefore, the selected self-saturation term can represent the d-q axis self-saturation through appropriate A, B, and C.

B. Proposed Flux Saturation Model including Cross-Saturation Term

There are three conditions to consider when modeling the cross saturation term. First, the flux saturation model must satisfy the reciprocity condition. Second, when the orthogonal axis current is a constant value other than zero, the flux saturation model should show that the cross-saturation increases as the magnitude of the self-axis current increases, and then decreases. Lastly, when the self-axis current is constant, the flux saturation model should represent the phenomenon in which the cross saturation changes as the orthogonal axis current increases.

The flux saturation model that satisfies the first condition is expressed as

$$\psi_d(i_d,i_q) = \underbrace{A_d\,tan^{-1}(B_d i_d) + C_d i_d}_{\psi_{d,self}} + \underbrace{D'_{dq} f(i_d) \int g(i_q)\,di_q}_{\psi_{d,cross}}, \tag{6a}$$

$$\psi_q(i_d,i_q) = \underbrace{A_q\,tan^{-1}(B_q i_q) + C_q i_q}_{\psi_{q,self}} + \underbrace{D'_{dq} g(i_q) \int f(i_d)\,di_d}_{\psi_{q,cross}}, \tag{6b}$$

where, $f(i_d)$ is a function of i_d, $g(i_q)$ is a function of i_q, and D_{dq} is a variable for cross-saturation.

For (6), (3) is expressed as

$$\frac{d\psi_d(i_d,i_q)}{di_q} = \frac{d\psi_q(i_d,i_q)}{di_d} = D'_{dq} f(i_d) g(i_q), \tag{7}$$

Therefore, (6) satisfies the reciprocity condition.

To satisfy the second condition, $f(i_d)$ and $g(i_q)$ were selected as fractional functions, and K which determines the current at which cross-saturation is maximized was added to the denominator. In addition, the order of the numerator of $f(i_d)$ and $g(i_q)$ was selected to be one smaller than the order of the denominator so that $\int g(i_q)\,di_q$ and $\int f(i_d)\,di_d$ are natural logarithms. $f(i_d)$ and $g(i_q)$ satisfying second condition are expressed as

$$f(i_d) = \frac{i_d}{i_d^2 + K_d}, \tag{8a}$$

$$g(i_q) = \frac{i_q}{i_q^2 + K_q}. \tag{8b}$$

The derivative of $f(i_d)$ and $g(i_q)$ is as expressed as

$$\frac{\mathrm{d}f(i_d)}{\mathrm{d}i_d} = \frac{K_d - i_d^2}{(i_d^2 + K_d)^2}, \tag{9a}$$

$$\frac{\mathrm{d}g(i_q)}{\mathrm{d}i_q} = \frac{K_q - i_q^2}{(i_q^2 + K_q)^2}. \tag{9b}$$

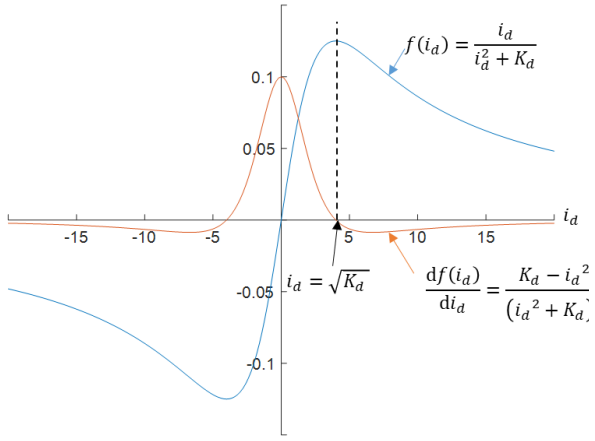

Fig. 3: $f(i_d)$ and $\mathrm{d}f(i_d)/\mathrm{d}i_d$ with respect to i_d

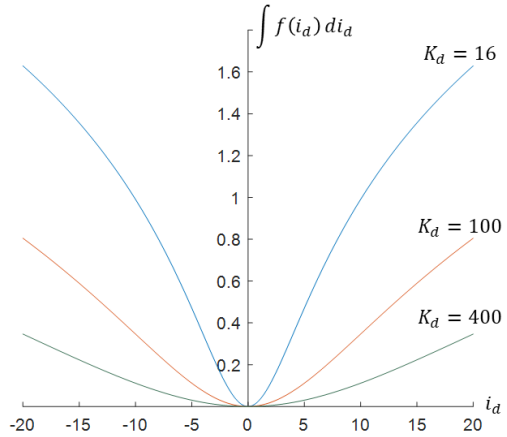

Fig. 4: $\int f(i_d)\, di_d$ according to K_d

As shown in Fig. 3, (8a) becomes maximum at the d axis current where equation (9a) becomes zero. And, the current at which (8a) becomes the maximum is $\sqrt{K_d}$. Therefore, the current at which the maximum cross saturation of the flux saturation model occurs is determined according to K_d.

The integral value with respect to the current in (8) is expressed as

$$\int f(i_d)\, di_d = \frac{1}{2}\ln\left(1 + \frac{i_d^2}{K_d}\right), \tag{10a}$$

$$\int g(i_q)\, di_q = \frac{1}{2}\ln\left(1 + \frac{i_q^2}{K_q}\right). \tag{10b}$$

Fig. 4 shows $\int f(i_d)\, di_d$ according to K_d. $\mathrm{d}\{\int f(i_d)\, di_d\}/\mathrm{d}i_d$ decreases as i_d increases when K_d is 16, and increases as i_d increases when K_d is 400. Therefore, the flux saturation model can satisfy the third condition according to K_d.

The proposed flux saturation model considering the above three conditions is expressed as

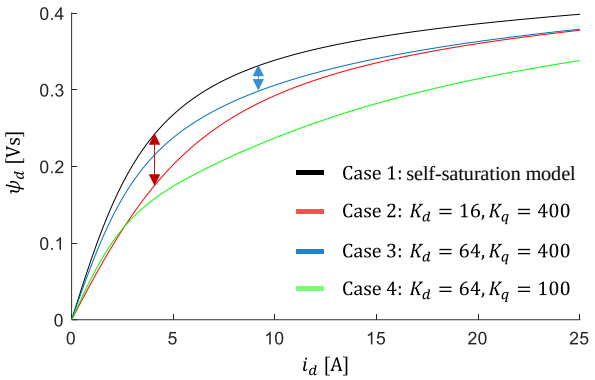

Fig. 5: D-axis flux saturation model according to K_d and K_q when D_{dq} and i_q are constant.

$$\psi_d(i_d, i_q) = \underbrace{A_d\, tan^{-1}(B_d i_d) + C_d i_d}_{\psi_{d,self}} + \underbrace{D_{dq}\frac{i_d}{i_d^2 + K_d}\ln\left(1 + \frac{i_q^2}{K_q}\right)}_{\psi_{d,cross}}, \tag{11a}$$

$$\psi_q(i_d, i_q) = \underbrace{A_q\, tan^{-1}(B_q i_q) + C_q i_q}_{\psi_{q,self}} + \underbrace{D_{dq}\frac{i_q}{i_q^2 + K_q}\ln\left(1 + \frac{i_d^2}{K_d}\right)}_{\psi_{q,cross}}. \tag{11b}$$

where, K_d, K_q, and D_{dq} are parameters for cross-saturation.

Fig. 5 shows an example d-axis flux saturation model according to the parameters for cross saturation. Case 1 is a self-saturation model, and the other cases are flux saturation models including cross-saturation in Fig. 5. K_d of case 2 and case 3 are 16 and 64, respectively. The d-axis current at which the maximum difference between case1 and case 2 occurs is 4 A, and the d-axis current at which the maximum difference between case1 and case 3 occurs is 8 A. Therefore, a cross-saturation phenomenon according to the d-axis current can be represented according to K_d. Case 4 has a smaller K_q than case 3, and cross-saturation increased for the same q-axis current. K_q determines the cross-saturation according to the q-axis current. Similarly, K_q in (11b) determines the q-axis current at which cross-saturation occurs at the maximum, and K_d determines the cross-saturation according to the d-axis current.

V. Experimental Result

The proposed flux saturation model was experimentally verified for a 1.5 kW SynRM. Table I gives the values on the test motor's nominal parameters. The DC-link voltage of the inverter was 310 V. The switching frequency was set at 5 kHz, and a double sampling method was used. A dead-time voltage distortion compensation algorithm was applied to reduce the error between the voltage reference

TABLE I
NOMINAL PARAMETERS OF THE 1.5 KW SYNRM

Parameter	Value [Unit]
Rated power	1.5 [kW]
Pole pair	2
Rated speed	3000 [r/min]
Rated Voltage	210 [$V_{L-L,RMS}$]
Rated Current	7.5 [A_{RMS}]
Inertia	0.0245 [kg · m^2]

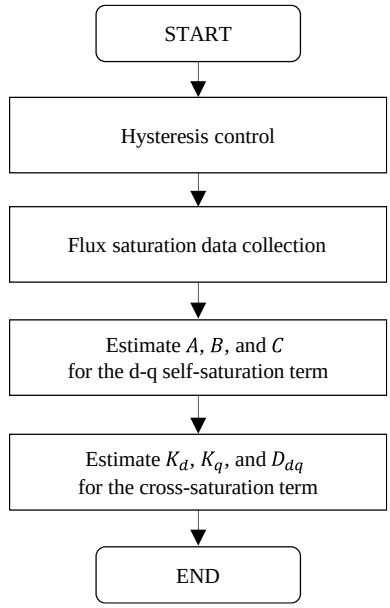

Fig. 6: Flow chart of flux saturation data collection and parameters estimation of the proposed flux saturation model.

TABLE II
ESTIMATED PARAMETERS OF THE PROPOSED FLUX SATURATION MODEL FOR 1.5 KW SYNRM

A_d	B_d	C_d	A_q	B_q	C_q	K_d	K_q	D_{dq}
0.26	0.32	0.0009	0.02	1.55	0.007	7	66	-0.12

and the actual output voltage of the inverter due to the dead-time voltage distortion. The hysteresis voltage injection method [5] obtained data on d-q axis self-saturation and cross-saturation. Fig. 6 shows the flow chart for flux saturation data collection and MATLAB curve fitting based on the nonlinear least square algorithm. The flux saturation model estimated through the root mean squared error (RMSE) was evaluated.

A. Self-saturation Terms

The black dots are the flux data obtained through the hysteresis voltage injection process, and the blue line is the estimated flux saturation model in Fig. 7. The parameters of the estimated d-q axis self-saturation model are shown in Table 2. Fig. 7(a) shows that the estimated d-axis flux saturation model represents the d-axis self-saturation data well where flux saturation appears significantly. In addition, Fig. 7(b) shows that the estimated q-axis flux saturation model well represents the q-axis self-saturation in the case where flux saturation hardly appears. Fig. 8 shows the arctangent function and the linear function of

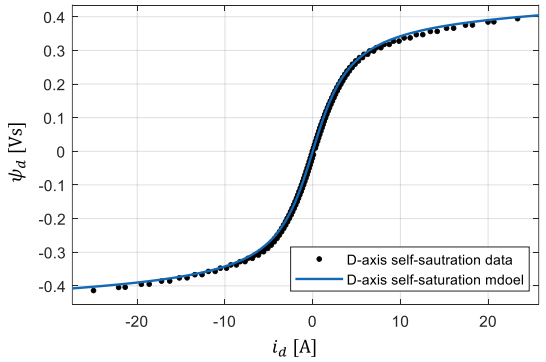

(a)

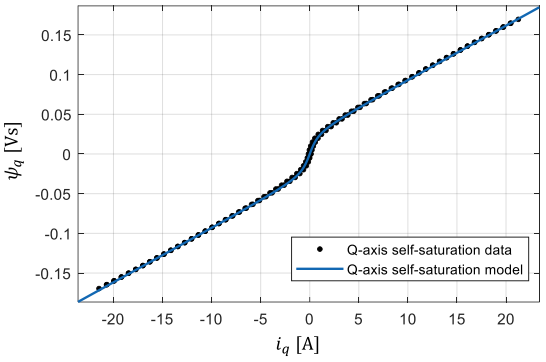

(b)

Fig. 7: Flux data and estimated self-saturation model using curve fitting tool of MATLAB: (a) d-axis self-saturation model and flux data; (b) q-axis self-saturation model and flux data.

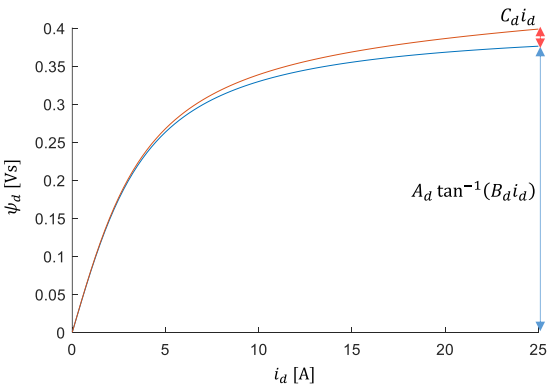

(a)

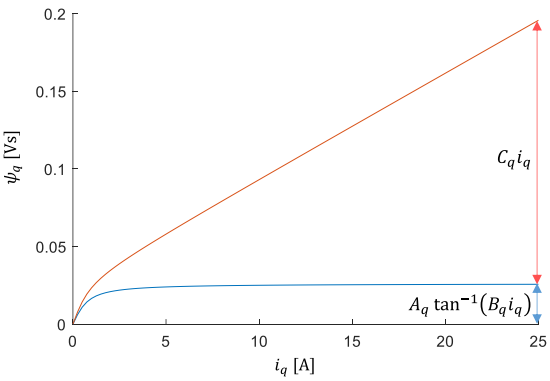

(b)

Fig. 8: Each term in the d-q axis self-saturation model estimated using the curve fitting tool in MATLAB: (a) d-axis; and (b) q-axis.

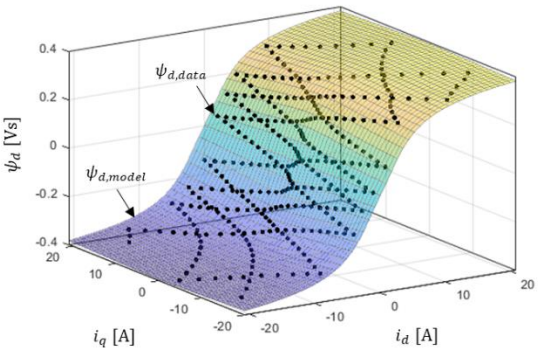

(a)

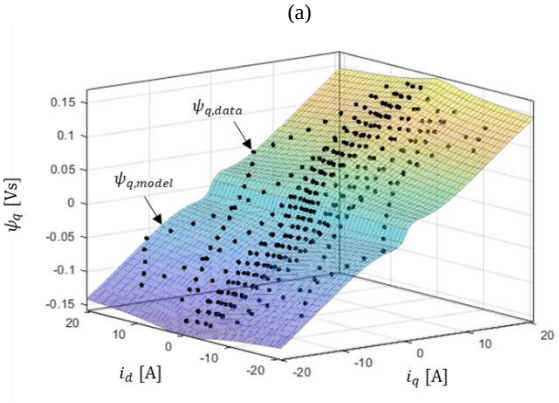

(b)

Fig. 9: Estimated d-q axis cross-saturation model using curve fitting tool of MATLAB.

the estimated self-saturation term. As explained in the section IV, the arctangent function represents the linear region and the smoothness around the knee point, and the linear function represents the saturation region.

B. Flux Saturation Model including Cross-saturation Terms

The black dots are the cross saturation data and the mesh plane shows the estimated d-q axis flux saturation model in Fig. 9. It was confirmed that the estimated flux saturation model well represented the flux saturation phenomenon of SynRM. Also, the RMSE between the estimated d-axis flux saturation model and d-axis flux data is 0.021, and the RMSE between the estimated q-axis flux saturation model and q-axis flux data is 0.009.

VI. Conclusion

This paper analyzes the flux saturation of SynRM and proposes a flux saturation model based on it. The proposed flux saturation model consists of a self-saturation term and a cross-saturation term, and the meaning of each parameter is explained. Also, this model satisfies the reciprocity condition. For the flux saturation of a 1.5 kW SynRM obtained through experiments, the parameters of the flux saturation model were estimated using MATLAB. And, it was confirmed that the estimated flux saturation model represents the flux saturation of the 1.5 kW SynRM well.

Acknowledgment

This paper was supported by Korea Institute for Advancement of Technology(KIAT) grant funded by the Korea Government(MOTIE)
(P0017120, The Competency Development Program for Industry Specialist)

References

[1] C. Mademlis, “Compensation of magnetic saturation in maximum torque to current vector controlled synchronous reluctance motor drives”, IEEE Transactions on Energy Conversion, vol. 18, no. 3, pp. 379-385, 2003.

[2] M. N. Ibrahim, E. M. Rashad and P. Sergeant, "Transient analysis and stability limits for synchronous reluctance motors considering saturation effects," 2015 18th International Conference on Electrical Machines and Systems (ICEMS), 2015, pp. 1812-1816.

[3] C. Mademlis, “Compensation of magnetic saturation in maximum torque to current vector controlled synchronous reluctance motor drives”, IEEE Transactions on Energy Conversion, vol. 18, no. 3, pp. 379-385, 2003.

[4] P. Guglielmi, M. Pastorelli and A. Vagati, "Impact of cross-saturation in sensorless control of transverse-laminated synchronous reluctance motors," in IEEE Transactions on Industrial Electronics, vol. 53, no. 2, pp. 429-439, April 2006.

[5] S. -W. Park, T. -G. Woo, S. -C. Choi, H. -J. Lee and Y. -D. Yoon, "Mitigating Rotor Movement During Estimation of Flux Saturation Model at Standstill for IPMSMs and SynRMs," in IEEE Transactions on Industrial Electronics, vol. 70, no. 2, pp. 1171-1181, Feb. 2023.

[6] I. Nasui-Zah, A. -H. Tamas and C. -S. Martis, "Impact of saturation and cross-saturation on SynRM's dynamic model," 2019 15th International Conference on Engineering of Modern Electric Systems (EMES), Oradea, Romania, 2019, pp. 145-148.

[7] Shoujun Song, Lefei Ge, Shaojie Ma, Man Zhang, "Accurate modeling of switched reluctance machine based on hybrid trained WNN," in AIP Advances, vol. 4, no. 4, April 2014.

[8] M. R. Raia, M. Ruba, R. O. Nemes and C. Martis, "Artificial Neural Network and Data Dimensionality Reduction Based on Machine Learning Methods for PMSM Model Order Reduction," in IEEE Access, vol. 9, pp. 102345-102354, 2021.

[9] M. Hinkkanen, P. Pescetto, E. Mölsä, S. E. Saarakkala, G. Pellegrino and R. Bojoi, "Sensorless Self-Commissioning of Synchronous Reluctance Motors at Standstill Without Rotor Locking," in IEEE Transactions on Industry Applications, vol. 53, no. 3, pp. 2120-2129, May-June 2017.

[10] K. A. Corzine, B. T. Kuhn, S. D. Sudhoff and H. J. Hegner, "An improved method for incorporating magnetic saturation in the q-d synchronous machine model," in IEEE Transactions on Energy Conversion, vol. 13, no. 3, pp. 270-275, Sept. 1998.

[11] N. Bedetti, S. Calligaro and R. Petrella, "Stand-Still Self-Identification of Flux Characteristics for Synchronous Reluctance Machines Using Novel Saturation Approximating Function and Multiple Linear Regression," in IEEE Transactions on Industry Applications, vol. 52, no. 4, pp. 3083-3092, July-Aug. 2016.

[12] C. Perez-Rojas, “Fitting saturation and hysteresis via arctangent functions,” IEEE Power Eng. Rev., vol. 20, no. 11, pp. 55–57, Nov. 2000

[13] Y. Iwaji, J. Nakatsugawa, T. Sakai, S. Aoyagi and H. Nagura, "Motor drive system using nonlinear mathematical model for permanent magnet synchronous motors," 2014 International Power Electronics Conference (IPEC-Hiroshima 2014 - ECCE ASIA), Hiroshima, 2014, pp. 2451-2456.

[14] A. Accetta, M. Cirrincione, M. Pucci and A. Sferlazza, "A Saturation Model of the Synchronous Reluctance Motor and its Identification by Genetic Algorithms," 2018 IEEE Energy Conversion Congress and Exposition (ECCE), Portland, OR, USA, 2018, pp. 4460-4465.